Excitation Spectrum of Arsenic Impurity in Germanium under Uniaxial Compression*

J. H. REUSZER AND P. FISHER
Department of Physics, Purdue University, Lafayette, Indiana
(Received 3 May 1965)

The effect of uniaxial stress on the excitation spectrum of arsenic impurity in germanium has been studied for compression along the simple directions [111], [110], and [100] using polarized light. The results can be understood in the framework of the effective-mass theory of Kohn and Luttinger and the deformation-potential theory. Selection rules for the observed transitions have been deduced from symmetry arguments. However, actual calculations of relative intensities of transitions are also given. Qualitative comparison of the latter with the observations gives good agreement.

I. INTRODUCTION

THE effect of a uniaxial stress on the energy states of Group V impurities in germanium has been determined by Price.[1] Similar calculations for silicon have been made by Wilson and Feher.[2] These latter authors have also determined the new ground-state wave functions for the case of silicon while such calculations for germanium have also been made.[3–6] The functional behavior of the lower ground state of the Group V impurities in germanium and silicon under stress has been utilized to determine the chemical splittings of the ground states.[2,5–8] Direct optical determinations of the chemical splittings[9,10] have shown that the indirect determinations are correct, except for the case of antimony in germanium.[9] This type of agreement is evidence that the perturbation calculation is correct. Little experimental work has been done on Group V donors in germanium to determine whether the excited states behave in the manner that deformation-potential theory[11] and the effective-mass approximation[12] would predict. An extensive investigation of this behavior for silicon has been made recently by Aggarwal and Ramdas.[13] In the latter investigation, the stress-induced effects are determined from the behavior of the excitation spectrum of the impurity under uniaxial stress. This technique has proved very useful for studying lithium in silicon,[14] giving important information about the nature of the ground state of the impurity. Weinreich and White[8] have observed the splitting of the excitation lines of the Group V impurities in germanium due to a uniaxial stress. The object of such measurements was to deduce the chemical splittings of the ground states of these impurities. The observations did not utilize polarized light and thus did not permit any detailed conclusions to be drawn regarding the excited states. A preliminary account, by the present authors, of the behavior of the spectrum of arsenic impurity in germanium under stress, using polarized light, has been given elsewhere.[15] A more detailed account of this work is presented here.

II. EXPERIMENTAL PROCEDURE

An oriented sample of arsenic-doped germanium was cut from an ingot which was known to be reasonably free from other Group V impurities.[9] After grinding and etching, the sample was inserted into a differential thermal contraction strain jig.[16] The jig and sample were then clipped to the copper tailpiece of an optical cryostat.[17] For improved thermal contact between the assembly and the tailpiece, short copper leads were soldered to the jig and then to the tailpiece. In some instances, copper leads were also connected between the ends of the sample and the tailpiece. Upon cooling, the sample and the copper jig contract by different amounts thus subjecting the sample to a uniaxial compression which, by design, was longitudinal. Using the known magnitudes of the linear coefficients of expansion of germanium[18] and copper,[19] it is estimated that the

* Work supported in part by the Advanced Research Projects Agency and by a U. S. Office of Naval Research Contract.

[1] P. J. Price, Phys. Rev. **104**, 1223 (1956).
[2] D. K. Wilson and G. Feher, Phys. Rev. **124**, 1068 (1961).
[3] H. Fritzsche, Phys. Rev. **119**, 1899 (1960).
[4] H. Fritzsche, Phys. Rev. **125**, 1560 (1962).
[5] D. K. Wilson and G. Feher, Bull. Am. Phys. Soc. **5**, 60 (1960); and G. Feher, *Proceedings of the International Conference on Semiconductor Physics, Prague 1960* (Czechoslovak Academy of Sciences, Prague, 1961), p. 579.
[6] D. K. Wilson, Phys. Rev. **134**, A265 (1964).
[7] H. Fritzsche, Phys. Rev. **115**, 336 (1959); **120**, 1120 (1960).
[8] G. Weinreich and H. G. White, Bull. Am. Phys. Soc. **5**, 60 (1960); and G. Weinreich, *Proceedings of the International Conference on Semiconductor Physics, Prague 1960* (Czechoslovak Academy of Sciences, Prague, 1961), p. 360.
[9] P. Fisher, J. Phys. Chem. Solids **23**, 1346 (1962); J. H. Reuszer and P. Fisher, Phys. Rev. **135**, A1125 (1964).
[10] R. L. Aggarwal, Solid State Commun. **2**, 163 (1964).
[11] C. Herring, Bell System Tech. J. **34**, 237 (1955); C. Herring and E. Vogt, Phys. Rev. **101**, 944 (1956).
[12] W. Kohn, *Solid State Physics*, edited by F. Seitz and D. Turnbull (Academic Press Inc., New York, 1957), Vol. 5, p. 257.
[13] R. L. Aggarwal and A. K. Ramdas, Phys. Rev. **137**, A602 (1965); and *Proceedings of the International Conference on the Physics of Semiconductors, Paris 1964* (Dunod Cie., Paris, 1964), p. 797.
[14] R. L. Aggarwal, P. Fisher, V. Mourzine, and A. K. Ramdas, Phys. Rev. **138**, A882 (1965).
[15] J. H. Reuszer and P. Fisher, Bull. Am. Phys. Soc. **9**, 645 (1964).
[16] A. C. Rose-Innes, Proc. Phys. Soc. (London) **72**, 514 (1958).
[17] P. Fisher, W. H. Haak, E. J. Johnson, and A. K. Ramdas, *Proceedings of the Eighth Symposium on the Art of Glassblowing* (The American Scientific Glassblowers Society, Wilmington, Delaware, 1963), p. 136.
[18] D. F. Gibbons, Phys. Rev. **112**, 136 (1958).
[19] D. Bijl and H. Pullan, Physica **21**, 285 (1955).

maximum strain obtainable in this way is $\sim 10^{-3}$. However, owing to slippage between the sample and jig, such strains were never attained. In fact, in the present investigation, to enable unambiguous identification to be made of the stress-induced line components, only small strains were desired. Such strains were achieved by selecting a suitable grease[16] to bond the sample to the jig.

The optical cryostat was mounted in a grating spectrometer with an image of the exit slit formed on the sample. The instrument was equipped with a Golay detector with a wedged crystalline quartz window. A Bausch and Lomb diffraction grating blazed for 112 micron was used in the 98G Perkin-Elmer monochromator. The sample was cooled with the use of liquid helium and the absorption spectra examined using

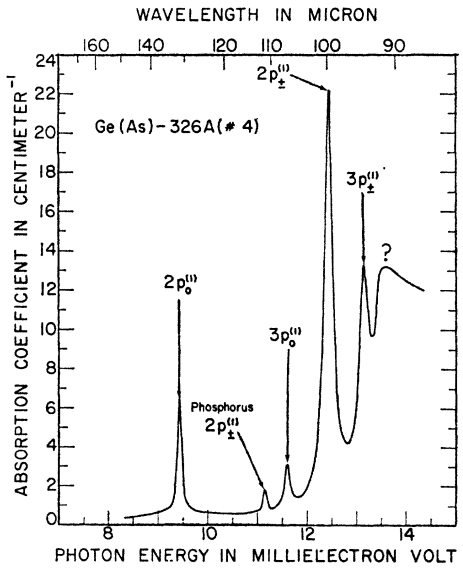

FIG. 1. The excitation spectrum of arsenic-doped germanium at $\sim 7°$K. $N(\text{As}) \simeq 1.2 \times 10^{15}$ cm^{-3}.

polarized light with **E**, the electric vector, either parallel or perpendicular to the compressive force, **F**[20]; these two arrangements will be designated by $\mathbf{E}_{\parallel}$ and $\mathbf{E}_{\perp}$, respectively. The light was polarized by the use of a polyethylene polarizer[21] located in front of the entrance slit of the monochromator.

III. EXPERIMENTAL RESULTS

The absorption spectrum of arsenic impurity in germanium shown in Fig. 1 was examined with **F**

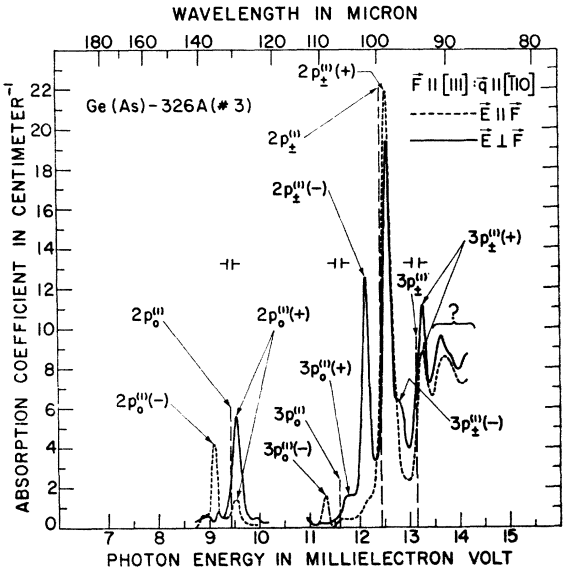

FIG. 2. The effect of a [111] compression on the excitation spectrum of arsenic in germanium at $\sim 8°$K. The dashed curve is for $\mathbf{E}_{\parallel}$ while the full curve is for $\mathbf{E}_{\perp}$. The vertical dashed lines indicate the energies of the zero-stress transitions. $N(\text{As}) \simeq 0.8 \times 10^{15}$ cm^{-3}.

parallel to the simple crystallographic directions [111], [110], and [100]. These data are given in Figs. 2, 3, 4, and 5; the vertical dashed lines show the positions of the zero stress excitation lines of Fig. 1. For $\mathbf{F} \| [110]$, the effects for two directions of light propagation, **q**, were

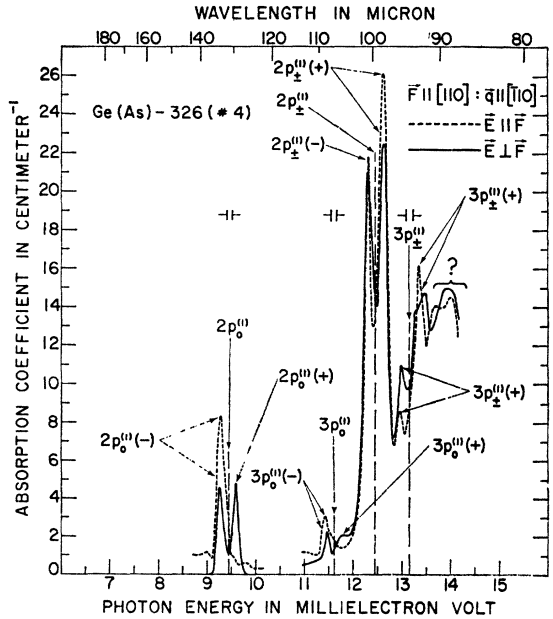

FIG. 3. The effect of a [110] compression on the excitation spectrum of arsenic in germanium at $\sim 8°$K for $\mathbf{q} \| [\bar{1}10]$, where **q** is the direction of light propagation. The dashed curve is for $\mathbf{E}_{\parallel}$ while the full curve is for $\mathbf{E}_{\perp}$. The vertical dashed lines indicate the energies of the zero-stress transitions. $N(\text{As}) \simeq 1.2 \times 10^{15}$ cm^{-3}.

[20] Crystalline quartz was used for windows on the cryostat. This material possesses a large optical rotation at short wavelengths. It was established that, in the range of wavelengths of the present measurements, the optical rotation of crystalline quartz is $<2°$ per mm.

[21] A. Mitsuishi, Y. Yamada, S. Fujita, and H. Yoshinaga, J. Opt. Soc. Am. **50**, 433 (1960).

studied, viz. $\mathbf{q}\|[\bar{1}10]$ (Fig. 3) and $\mathbf{q}\|[001]$ (Fig. 4). The data for the lower curve of Fig. 5, $\mathbf{F}\|[100]$, were taken using unpolarized light; it is quite clear that no splittings of the excitation lines occur. The upper curves of Fig. 5 show the polarization behavior of the two central lines under the same [100] compression.

In the above figures, the lines have been labelled in such a way as to indicate which states have participated in each transition, e.g., the strongest line (previously designated[9] as B_1) is due to a transition from the lower (or singlet) ground state to the $2p_\pm$ state, consequently this line has been labelled as $2p_\pm^{(1)}$. In addition, the stress induced components are designated according to whether they occur at a higher or a lower energy than the original line. In all cases, no more than two such components were observed for each zero-stress line, for example, for $\mathbf{F}\|[111]$ and $\mathbf{E}_\perp$ there is a $2p_0^{(1)}(+)$ component, while for $\mathbf{E}_\|$ there is a $2p_0^{(1)}(-)$ component as well as the $2p_0^{(1)}(+)$ component.

The results given were obtained at sample temperatures low enough to suppress transitions arising from the upper ground state thus avoiding any confusion between the stress components of $3p_\pm^{(3)}$, $2p_\pm^{(3)}$, and $2p_0^{(1)}$. It should be noted, however, that of the four Group V donors, arsenic should be the most convenient for studying the effect of stress on the triplet ground state. In view of the method used to achieve the uniaxial compression, a fine control of the strain was not possible, thus some difficulty was experienced in obtaining a strain large enough to split the lines adequately and yet permit the $3p_0^{(1)}(+)$ and $3p_\pm^{(1)}(-)$ lines to be resolved from the intense $2p_\pm^{(1)}$ components. This difficulty is

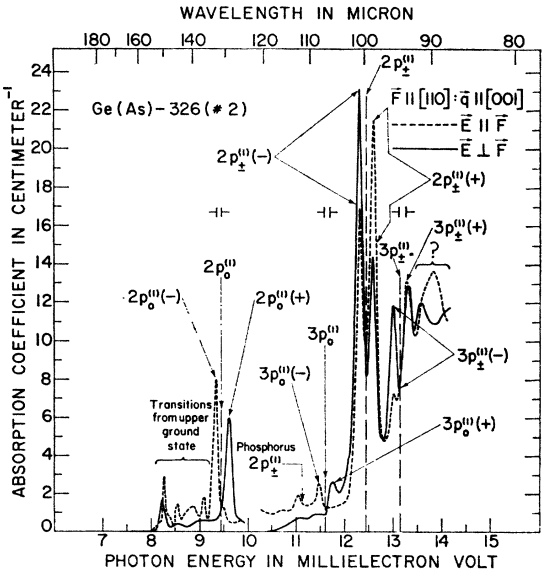

FIG. 4. The effect of a [110] compression on the excitation spectrum of arsenic in germanium at ~10°K for $\mathbf{q}\|[001]$. The dashed curve is for $\mathbf{E}_\|$ while the full curve is for $\mathbf{E}_\perp$. The vertical dashed lines indicate the energies of the zero-stress transitions. $N(\text{As})\simeq 1.1\times10^{15}$ cm^{-3}.

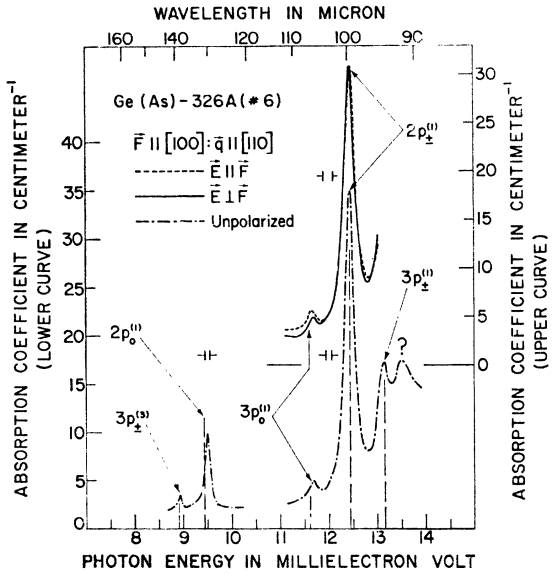

FIG. 5. The effect of a [100] compression on the excitation spectrum of arsenic in germanium at ~10°K. The lower curve was measured using unpolarized light. The upper curves show the two central lines for the two indicated directions of polarization. The vertical dashed lines are at the energies of the zero-stress transitions. $N(\text{As})\simeq 1.4\times10^{15}$ cm^{-3}.

most evident in Fig. 2; the reason for labeling the high-energy shoulder of the $2p_\pm^{(1)}(+)$ component as $3p_\pm^{(1)}(-)$ will become evident in the discussion. Some phosphorus was present in the ingot used as is indicated in Fig. 1. The extent to which the $2p_\pm^{(1)}$ transition of the phosphorus influences the $3p_0^{(1)}(-)$ transitions of the arsenic has not been determined. The regions of absorption designated by the question marks in all the spectra are due to unclassified transitions[9] which have not been investigated in any detail. In Fig. 3, the shape of the $3p_\pm^{(1)}(+)$ component for $\mathbf{E}_\perp$ may be influenced by these latter transitions.

IV. DISCUSSION

The spectra of Figs. 2–4 show that each line splits into two. This effect and the lack of splitting for $\mathbf{F}\|[100]$, Fig. 5, can be understood from the deformation potential theory when used to describe the behavior of the conduction band of a multivalley semiconductor under stress,[11] and by the effective-mass approximation.[12] The complete polarization of some of the components may be readily understood from symmetry arguments, while the relative intensities of the components of each original line can be calculated explicitly from the results of the effective mass formalism.

(i) Deformation Potential Theory

A convenient form of the equation for the shift in energy, ϵ_j, due to strain of the jth minimum relative to the center of gravity of the energies of the conduction

band minima, has been given by Keyes and Sladek,[22] viz.,

$$\epsilon_j = \pm \Xi_u |T| / 2C_{44} [(\hat{z}_j \cdot \mathbf{b})^2 - \tfrac{1}{3}], \quad (1)$$

where $\hat{z}_j$ is a unit vector along the axis of the jth $\langle 111 \rangle$ type of valley and $\mathbf{b}$ is the unit vector defining the direction of $\mathbf{F}$ which produces the stress, T. The quantities Ξ_u and C_{44} are the shear deformation potential constant[11] and one of the elastic stiffness constants, respectively. The positive sign is for tension and the negative sign for compression. For the three directions of compression examined, Eq. (1) gives[3,4]:

$$\begin{aligned} &\text{(a)} \quad \mathbf{F}\|[111]: \quad \epsilon_1 = -3\epsilon_a; \quad \epsilon_{2,3,4} = +\epsilon_a, \\ &\text{(b)} \quad \mathbf{F}\|[110]: \quad \epsilon_{1,3} = -\epsilon_b; \quad \epsilon_{2,4} = +\epsilon_b, \\ &\text{(c)} \quad \mathbf{F}\|[100]: \quad \epsilon_{1,2,3,4} = 0, \end{aligned} \quad (2)$$

where

$$\epsilon_a = \Xi_u |T| / 9C_{44} \quad \text{and} \quad \epsilon_b = \Xi_u |T| / 6C_{44},$$

the valleys being labelled in the following manner: 1—[111], 2—[1$\bar{1}\bar{1}$], 3—[$\bar{1}$11], and 4—[$\bar{1}$1$\bar{1}$].

(ii) Effective-Mass Theory

If it is assumed that both the dielectric constant and the effective masses characterizing the conduction band are unaltered by a small strain, then, for a given valley, the energy-level scheme of a Group V donor will be unaffected by the stress as the effective mass equation[12] for the jth valley will be unaltered. However, the energy-level schemes bearing different valley labels will be shifted relative to each other by the amounts given in Eq. (1). This will be true for all states which are well described by the effective-mass Hamiltonian, viz., the p states. For the ground state, this will not be so as it is well known that the potential used in the effective-mass wave equation is incorrect for this state. Price[1] has considered explicitly the effect of strain on the ground states of a shallow donor in germanium.

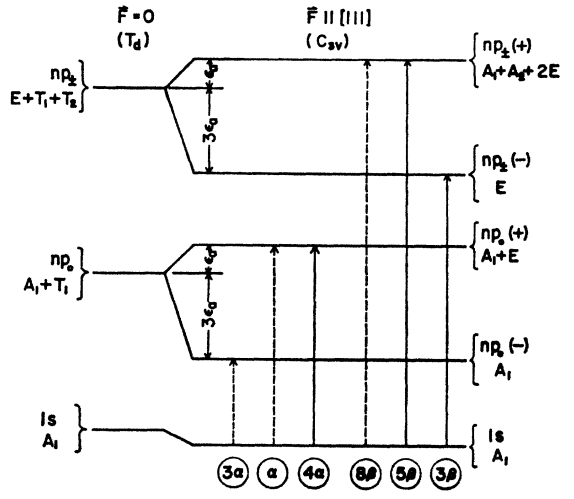

FIG. 6. Splitting of the shallow donor states in germanium under a [111] compression. The vertical arrows indicate the allowed transitions where the dashed arrows are for $\mathbf{E}_\parallel$ and the full arrows are for $\mathbf{E}_\perp$. The capital letters labelling the levels denote the irreducible representations of T_d and C_{3v} to which the states belong. Note that T_1 here is the irreducible representation under which x, y, and z transform. The quantity ϵ_a is defined in the text. The encircled quantity below each arrow refers to the intensity of the transition where $\alpha = A^2/12$ and $\beta = B^2/6$. The quantities A and B are defined in the Appendix, Eqs. (A6).

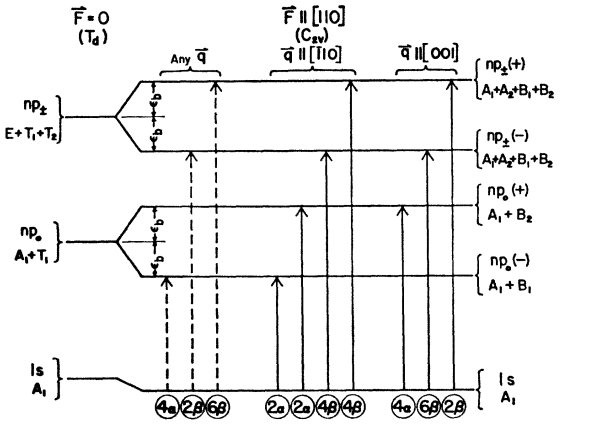

FIG. 7. Splitting of the shallow donor states in germanium under a [110] compression for $\mathbf{q}\|[\bar{1}10]$ and $\mathbf{q}\|[001]$. The allowed transitions are indicated by the vertical arrows, the dashed arrows are for $\mathbf{E}_\parallel$ while the full arrows are for $\mathbf{E}_\perp$. The remaining quantities are defined in a similar way to the quantities defined in the caption to Fig. 6.

The effect of a uniaxial compression on the energy scheme of a Group V donor in germanium, for $\mathbf{F}\|[111]$ and $\mathbf{F}\|[110]$, is shown in Figs. 6 and 7, respectively. The above prediction that each excited state splits into two levels (see also Ref. 8), while the lower (or singlet) ground state merely shifts, is in agreement with the data given in Figs. 2–4. Further, the disposition of the stress induced components about the original lines can now be understood. Neglecting the nonlinear shift of the ground state,[1] Eqs. (2) show that for $\mathbf{F}\|[111]$ all the low-energy components of the lines should be displaced three times farther from each original line than the high-energy components, while the spacing of the two components of each line should be $4\epsilon_a$. Similarly, for $\mathbf{F}\|[110]$ the high- and low-energy components of each line should be separated by $2\epsilon_b$, the components being symmetrically located about the original lines. These conclusions are borne out by the experimental observations, a summary of which is given in Table I. From the data for ϵ_a and ϵ_b, and the known values of Ξ_u[7,9] and C_{44},[23] the values shown for $|T|$ have been calculated. Also, from ϵ_a, ϵ_b, the chemical splitting[9] and the equations of Price,[1] an estimate was made of the shifts of the ground state; for the present cases these are negligible as was assumed above. In the case of $\mathbf{F}\|[100]$, Eqs. (2)

[22] R. W. Keyes and R. J. Sladek, Phys. Rev. **125**, 478 (1962).

[23] H. McSkimmin, J. Appl. Phys. **24**, 988 (1953); M. E. Fine, J. Appl. Phys. **24**, 338 (1953).

TABLE I. Displacements of stress components of excitation lines[a] of arsenic impurity in germanium.[b] Units are millielectron volt.[c]

Fig. No.	$2p_0(+)-2p_0$	$2p_0-2p_0(-)$	$3p_0(+)-3p_0$	$3p_0-3p_0(-)$	$2p_\pm(+)-2p_\pm$	$2p_\pm-2p_\pm(-)$	$3p_\pm(+)-3p_\pm$	$3p_\pm-3p_\pm(-)$	$\bar{\epsilon}_{a,b}$	$\lvert T\rvert \times 10^{-7}$ (dyne/cm^2)
2	0.11	0.32	~0.13	0.29	0.12	0.31	0.12	~0.31	0.11	3.5
3	0.16	0.17	0.15	0.16	0.18	0.14	0.19	0.17	0.16	3.4
4	0.17	0.11	0.14	0.14	0.14	0.14	0.15	0.14	0.14	3.0

[a] All lines considered are due to transitions from the singlet ground state; hence the superscript (1) has been omitted from all labels.
[b] The column labelled $\bar{\epsilon}_{a,b}$ gives the average value of ϵ_a or ϵ_b as obtained from the displacements. ϵ_a and ϵ_b are defined in the text.
[c] The experimental error in the displacements is ±0.03 unit.

show that the valleys do not become energetically separated and thus no splitting is expected, in agreement with the experimental data of Fig. 5.

(iii) Selection Rules

In Figs. 6 and 7 are also shown the selection rules for the various transitions for **F**‖[111] and **F**‖[110], respectively. These rules may be determined from symmetry considerations. The symmetry of the impurity site under the applied stress may be obtained by enquiring as to which of the original symmetry elements now remain.[13,24] Once the new site symmetry has been found, the reduction of the old states into the new, may be accomplished by the technique described by Ramdas, Lee, and Fisher.[25] The results of such a decomposition are shown in Table II for **F**‖[111] and **F**‖[110]. The levels in Figs. 6 and 7 have been labelled according to the results given in Table II. With this information and using standard group theoretical techniques[26] the selection rules for electric dipole transitions were deduced.

A detailed comparison of the selection rules with the experimental data, shows that the two are in exact agreement. The origin of the differences between the two spectra for **F**‖[110], Figs. 3 and 4, may now be understood. Clearly, for $\mathbf{E}_{\perp}$, the spectrum should be independent of **q**. However, from Fig. 8, it is seen that

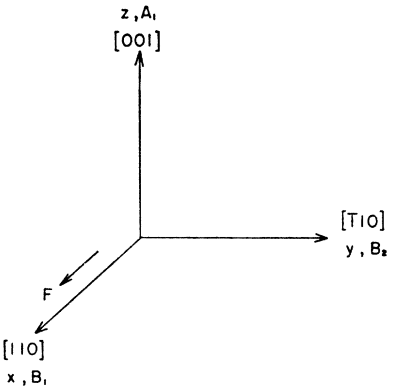

FIG. 8. The orthogonal axes of a cubic crystal under a [110] compression. The capital letters labelling the axes refer to the irreducible representations of the orthorhombic point group C_{2v} according to which x, y, and z transform.

the transformation properties of the electric-dipole moment are quite different for the two axes designated by y and z. This is indicated by the labels B_2 and A_1

TABLE II. Symmetry classification of shallow donor levels in germanium under an applied uniaxial force.

Direction of compression	Symmetry of impurity	Symmetry of valleys[a]	m	$\Gamma(C_{\infty v})$ $F=0$	Γ (valley) $F\neq 0$	Γ (impurity) $F\neq 0$	Level scheme $F=0$	Level scheme $F\neq 0$	
[111]	C_{3v}	$C_s(2,3,4)$	0	A_1	A'	A_1+E	A_1+T_1	A_1+E	(2,3,4)
		$C_{3v}(1)$			A_1	A_1		A_1	(1)
		$C_s(2,3,4)$	±1	E_1	$A'+A''$	A_1+A_2+2E	$E+T_1+T_2$	A_1+A_2+2E	(2,3,4)
		$C_{3v}(1)$			E	E		E	(1)
[110]	C_{2v}	$C_s(2,4)$	0	A_1	A'	A_1+B_2	A_1+T_1	A_1+B_2	(2,4)
		$C_s(1,3)$			A'	A_1+B_1		A_1+B_1	(1,3)
		$C_s(2,4)$	±1	E_1	$A'+A''$	$A_1+A_2+B_1+B_2$	$E+T_1+T_2$	$A_1+A_2+B_1+B_2$	(2,4)
		$C_s(1,3)$			$A'+A''$	$A_1+A_2+B_1+B_2$		$A_1+A_2+B_1+B_2$	(1,3)

[a] The numbers in parentheses label the valleys and, in column three, indicate to which subgroup a given valley belongs. The valleys are numbered as follows: 1—[111], 2—[1$\bar{1}\bar{1}$], 3—[$\bar{1}$11], and 4—[$\bar{1}1\bar{1}$].

[24] H. S. Peiser, J. B. Wachtman, Jr., and R. W. Dickson, J. Res. Natl. Bur. Std. **A67**, 395 (1963).
[25] A. K. Ramdas, P. M. Lee, and P. Fisher, Phys. Letters **7**, 99 (1963).
[26] See, for example, L. D. Landau and E. M. Lifshitz, *Quantum Mechanics*, translated by J. B. Sykes and J. S. Bell (Pergamon Press Ltd., London, 1958), p. 343.

attached to y and z, respectively; these labels designate the irreducible representations of the point group C_{2v} to which y and z belong.[27] Thus for $\mathbf{q}\|[\bar{1}10]$ and $\mathbf{E}_\perp$, the active dipole moment will transform as A_1 and transitions from the singlet $1s(A_1)$ ground state are permitted only to those states transforming as A_1. For $\mathbf{q}\|[001]$ and $\mathbf{E}_\perp$, the dipole transforms as B_2 and hence transitions from $1s(A_1)$ are only allowed to states belonging to B_2. The behavior, in this respect, of the shallow donors in germanium is identical to their behavior in silicon.[13] In the case of $\mathbf{F}\|[111]$, however, the electric dipole moment has the same symmetry for all directions in the plane normal to $\mathbf{F}$ and thus no dependence on $\mathbf{q}$ is to be expected.

(iv) Relative Intensities:

An equation has been derived by Kohn[12] which may be used to calculate the relative intensities of the two stress components which arise from each original line. This is discussed briefly in the Appendix and, of course, automatically gives the selection rules of the previous subsection. The latter has been included for completeness while the information given in Table II is particularly useful in deducing the wave functions of the states under stress. The results of the intensity calculations, in the limit of zero stress, are indicated by the encircled numbers below the transitions shown in Figs. 6 and 7. A comparison between these values and the experimental data of Figs. 2–4 shows that the agreement is good. In the case of $\mathbf{F}\|[111]$, and $\mathbf{E}_\|$, the intensities of the $2p_0^{(1)}(-)$ and $2p_0^{(1)}(+)$ transitions are predicted to be in the ratio of 3:1, while $2p_0^{(1)}(+)$ for $\mathbf{E}_\perp$ should be four times as intense as it is for $\mathbf{E}_\|$. This is in accord with the experimental data of Fig. 2. The same relative intensities are also predicted for the components of the weak $3p_0^{(1)}$ transitions; this too is in essential agreement with the experiment. For the $np_\pm^{(1)}$ transitions, it is predicted that for $\mathbf{E}_\perp$ the high energy component should be $\frac{5}{3}$ as intense as the low energy component while $np_\pm^{(1)}(+)$ for $\mathbf{E}_\perp$ should be only $\frac{5}{8}$ as intense as for $\mathbf{E}_\|$. These predictions are supported by the intensities of the $2p_\pm^{(1)}$ components. Some minor discrepancies may be due to errors in measuring the transmission of the sample at the peaks of the strong $2p_\pm^{(1)}$ components. The data for the $3p_\pm^{(1)}$ components do agree qualitatively with the predictions; when estimating intensities for this line it should be noted that there is a large background present. For the other direction of compression, Figs. 3 and 4, similar comparisons may be made between the theory and experiment, giving similar agreement.

ACKNOWLEDGMENTS

The authors wish to thank Professor A. K. Ramdas and Dr. R. L. Aggarwal for many useful discussions. They wish also to thank Professor R. C. Buschert, Professor H. J. Yearian, and Miss Louise Roth for orienting the crystals. They are indebted to A. Onton for use of the computer program in the analysis of the data.

APPENDIX

The momentum matrix elements for electric-dipole transitions between the ground state and an excited state of a shallow donor impurity in a multivalley semiconductor has been shown by Kohn[12] to be

$$M_{x_k}=(m/i\hbar)(E_e-E_{1s})\sum_{j=1}^{N}\alpha_{j,1s}{}^*\alpha_{je}(F_{j,1s},x_kF_{je}),$$

$$k=1,\ 2,\ \text{and}\ 3 \quad \text{(A1)}$$

where m is the inertial mass of the electron and E_e and E_{1s} are the energies of the two states. The coefficients $\alpha_{j,1s}$ and α_{je} are defined as follows: The wave function, Ψ of a given state is a linear combination of the product functions $F_j\varphi_j$, i.e.,

$$\Psi=\sum_{j=1}^{N}\alpha_jF_j\varphi_j, \quad \text{(A2)}$$

where the envelope function F_j is a solution of the jth effective mass equation[12] and φ_j is the Bloch function at the jth conduction band minimum; in the case of germanium, $N=4$.

The components of the valley matrix elements, $(F_{j,1s},x_kF_{je})$, may be written as follows:

$$\begin{aligned} m_{jx_k}&=m_\| \cos(x_k,z_j), \quad (np_0)\\ m_{jx_k}&=m_\perp[\cos(x_k,x_j)\pm i\cos(x_k,y_j)], \quad (np_\pm)\end{aligned} \quad \text{(A3)}$$

where x_j, y_j, and z_j define the coordinate system of the jth valley whose axis is z_j. The quantities $m_\|$ and $m_\perp$ are defined by

$$m_\|=C\int z_j^2\exp\left[-\left(\frac{x_j^2+y_j^2}{a_{1s}{}^2}+\frac{z_j^2}{b_{1s}{}^2}\right)^{1/2}-\left(\frac{x_j^2+y_j^2}{a_0^2}+\frac{z_j^2}{b_0^2}\right)^{1/2}\right]d\tau$$

and

$$m_\perp=D\int\begin{pmatrix}x_j^2\\ y_j^2\end{pmatrix}\exp\left[-\left(\frac{x_j^2+y_j^2}{a_{1s}{}^2}+\frac{z_j^2}{b_{1s}{}^2}\right)^{1/2}-\left(\frac{x_j^2+y_j^2}{a_\pm{}^2}+\frac{z_j^2}{b_\pm{}^2}\right)^{1/2}\right]d\tau.$$

Here the quantities a_{1s}, b_{1s}, a_0, b_0, $a_\pm$, and $b_\pm$ are measures of the sizes of the $1s$, np_0 and $np_\pm$ orbits, re-

[27] See Ref. 26, p. 338.

spectively, and C and D are constants related to the a's and b's.

Substitution of (A3) into (A1) yields

$$M_{x_k}(np_0)=\frac{A}{i}\sum_{j=1}^{4}\alpha_{j,1s}{}^{*}\alpha_{j,np_0}\cos(x_k,z_j)\,, \tag{A4}$$

$$M_{x_k}(np_\pm)=\frac{B}{i}[\sum_{j=1}^{4}\alpha_{j,1s}{}^{*}(\alpha_{j,np_+}+\alpha_{j,np_-})\cos(x_k,x_j)$$

$$+i\sum_{j=1}^{4}\alpha_{j,1s}{}^{*}(\alpha_{j,np_+}-\alpha_{j,np_-})\cos(x_k,y_j)], \tag{A5}$$

where

$$A=[m(E_0-E_{1s})m_{\parallel}]/\hbar\,,$$

and (A6)

$$B=[m(E_\pm-E_{1s})m_{\perp}]/\hbar\,.$$

If it is assumed that the F_j's are not seriously altered for small strain,[4] the problem of finding the intensities of the stress induced components reduces to determining the α's for the new wave functions. Simple group theoretical techniques enable this to be accomplished for the excited states. The new linear combination for the ground state[3,4,6] may be determined from Price's[1] results for the dependence of the energy of this state on strain. As an example, for $\mathbf{F}\|[111]$, the new site symmetry is C_{3v} and the new wave functions are as follows:

(i) p-Like States

$$\Psi(A_1)=(6)^{-1/2}(0,0,\omega^*,-\omega,1,-1,\omega,-\omega^*)\,,$$

$$\Psi(A_2)=(6)^{-1/2}(0,0,\omega^*,\omega,1,1,\omega,\omega^*)\,,$$

$$\Psi(E)=\tfrac{1}{2}(0,0,0,1,-\omega^*,-\omega^*,1,0) \qquad np_\pm(+)$$
$$=(12)^{-1/2}(0,0,2\omega,1,-\omega^*,\omega^*,-1,-2\omega)\,,$$

$$\Psi(E)=\tfrac{1}{2}(0,0,0,\omega^*,\omega,-\omega,-\omega^*,0)$$
$$=(12)^{-1/2}(0,0,2,-\omega^*,-\omega,-\omega,-\omega^*,2)\,,$$

$$\Psi(E)=(2)^{-1/2}(1,1,0,0,0,0,0,0) \qquad np_\pm(-)$$
$$=(2)^{-1/2}(1,-1,0,0,0,0,0,0)\,,$$

$$\Psi(A_1)=(3)^{-1/2}(0,1,1,1)\,,$$

$$\Psi(E)=(2)^{-1/2}(0,1,-1,0) \qquad np_0(+)$$
$$=(6)^{-1/2}(0,1,1,-2)\,,$$

$$\Psi(A_1)=(1,0,0,0)\,. \qquad np_0(-)$$

For the $p_\pm$ states the α_{j+} and α_{j-} alternate, with α_{j+} being first; also $\omega=\exp(2\pi i/3)$. The letter in parenthesis following Ψ indicates the irreducible representation of C_{3v} to which the state belongs.

(ii) Lowest Ground State

$$\Psi(A_1):\quad(\alpha_1,\alpha_2,\alpha_2,\alpha_2)\,,$$

where[4,28]

$$\alpha_1{}^2=1/4(2+\gamma)\quad\text{and}\quad\alpha_2{}^2=1/12(2-\gamma)\,.$$

Here

$$\gamma=(2\epsilon_a-\Delta_c)(\epsilon_a{}^2-\epsilon_a\Delta_c+\Delta_c{}^2)^{-1/2}\,,$$

and $4\Delta_c$ is the chemical splitting of the ground state; ϵ_a is defined in Sec. IV where the labelling of the valleys is also given. For the case of small stress, i.e., $\epsilon_a\ll\Delta_c$,

$\alpha_1{}^2\simeq(2+3\epsilon')/8$ and $\alpha_2{}^2\simeq(2-\epsilon')/8$, where $\epsilon'=\epsilon_a/\Delta_c$.

In this approximation, for example, the transitions $1s(A_1)\rightarrow 2p_0(+)$ and $1s(A_1)\rightarrow 2p_0(-)$, for the two directions of polarization have the intensities

$$I_{\parallel}(-)\propto\tfrac{1}{8}A^2(2+3\epsilon')\,;\qquad I_{\perp}(-)=0\,,$$
$$I_{\parallel}(+)\propto(A^2/24)(2-\epsilon')\,;\quad I_{\perp}(+)\propto\tfrac{1}{6}A^2(2-\epsilon')\,,$$

where the difference in (E_e-E_{1s}) for the two $2p_0$ levels has been neglected.

In the extreme limit of zero stress

$$I_{\parallel}(-)\propto\tfrac{1}{4}A^2;\quad I_{\perp}(-)=0\,,$$
$$I_{\parallel}(+)\propto\tfrac{1}{12}A^2;\quad I_{\perp}(+)=\tfrac{1}{3}A^2.$$

These latter values are those given in Fig. 6. All other intensities indicated in Figs. 6 and 7 have been determined using the zero-stress linear combination of the ground-state wave function, viz., $\frac{1}{2}(1,1,1,1)$.

---

[28] In Ref. 6, Eqs. (A16) and (B21) have an error in the sign of the quantity $8x/9$.